Allosteric Mechanisms in Cytochrome P450 3A4 Studied by High-Pressure Spectroscopy: Pivotal Role of Substrate-Induced Changes in the Accessibility and Degree of Hydration of the He...

ARTICLE *in* BIOCHEMISTRY · JULY 2007

Impact Factor: 3.02 · DOI: 10.1021/bi602400y · Source: PubMed

4 AUTHORS, INCLUDING:

Dmitri Davydov
University of California, San Diego
57 PUBLICATIONS **1,363** CITATIONS
SEE PROFILE

James R Halpert
University of Connecticut
238 PUBLICATIONS **9,314** CITATIONS
SEE PROFILE

Published in final edited form as:
Biochemistry. 2007 July 3; 46(26): 7852–7864. doi:10.1021/bi602400y.

Allosteric Mechanisms in Cytochrome P450 3A4 Studied by High-Pressure Spectroscopy: Pivotal Role of Substrate-Induced Changes in the Accessibility and Degree of Hydration of the Heme Pocket†

Dmitri R. Davydov[‡,*], **Bradley J. Baas**[§], **Stephen G. Sligar**[§], and **James R. Halpert**[‡]
Department of Pharmacology and Toxicology, The University of Texas Medical Branch, 301 University Blvd., Galveston, Texas 77555; Department of Biochemistry and Chemistry, Beckman Institute for Advanced Science and Technology, University of Illinois Urbana-Champaign, Urbana, Illinois 61801

Abstract

Allosteric mechanisms in human cytochrome P450 3A4 (CYP3A4) in oligomers in solution or monomeric enzyme incorporated into Nanodiscs (CYP3A4ND) were studied by high-pressure spectroscopy. The allosteric substrates 1-pyrenebutanol (1-PB) and testosterone were compared with bromocriptine (BCT), which shows no cooperativity. In both CYP3A4 in solution and CYP3A4ND we observed a complete pressure-induced high-to-low spin shift at pressures <3 kbar either in the substrate-free enzyme or in the presence of BCT. In addition, both substrate-free and BCT-bound enzyme revealed a pressure-dependent equilibrium between two states with different barotropic parameters designated “R” for relaxed and “P” for pressure-promoted conformations. This pressure-induced conformational transition was also observed in the studies with 1-PB and testosterone. In CYP3A4 oligomers the transition was accompanied by an important increase in homotropic cooperativity with both substrates. Surprisingly, at high concentrations of allosteric substrates the amplitude of the spin shift in both CYP3A4 in solution and in Nanodiscs was very low, demonstrating that hydrostatic pressure induces neither substrate dissociation nor an increase in heme pocket hydration in the complexes of the pressure-promoted conformation of CYP3A4 with 1-PB or testosterone. These findings suggest that the mechanisms of interactions of CYP3A4 with 1-PB and testosterone involve an effector-induced transition that displaces a system of conformational equilibria in the enzyme towards the state(s) with decreased solvent accessibility of the active site, so that water flux into the heme pocket is impeded, and the high-spin state of the heme iron is stabilized.

†This research was supported by NIH grants GM54995 (JRH), GM33775 (SGS), GM31756 (SGS), Center grant ES06676 (JRH), and Robert A. Welch Foundation grant H1458 (JRH).

* Corresponding author: E-mail: d.davydov@UTMB.edu. Tel.: (409) 772−9658; Fax: (409) 772−9642.
‡University of Texas Medical Branch
§University of Illinois Urbana-Champaign

Supporting information available.
The effect of hydrostatic pressure on tryptophan fluorescence of CYP3A4-containing Nanodiscs, the pressure-induced changes in the fluorescence of DCVJ incorporated into the Nanodiscs, the effect of HPCD on the interactions of 1-PB and testosterone with CYP3A4 and the effect of hydrostatic pressure on the fluorescence of 1-PB complexes with HPCD. These materials are available free of charge via the Internet at http://pubs.acs.org.

Keywords

cytochrome P450 3A4; bromocriptine; 1-pyrenebutanol; testosterone; substrate binding; spin equilibrium; cytochrome P420; protein hydration; hydrostatic pressure

Current advances in studies of substrate interactions of cytochromes P450 by biophysical techniques (1-3) and recently resolved X-ray structures of microsomal cytochromes P450 (4-6) have revealed an important conformational flexibility of cytochromes P450 3A4 (CYP3A4) and 2B4 (CYP2B4). The striking conformational rearrangements exhibited by these versatile drug-metabolizing enzymes are thought to play an important role in the adaptation of the geometry of the active site to a diverse set substrate structures. Further investigation of the molecular mechanisms and functional consequences of these conformational transitions are needed for a detailed understanding of the mechanisms of enzyme function. One of the most interesting questions in this regard is the role of the conformational flexibility in the mechanisms of homo- and heterotropic cooperativity exhibited by CYP3A4, the major human hepatic P450 enzyme, which is responsible for metabolism of a broad range of substrates of pharmacological and toxicological interest.

The prevailing hypothesis on the mechanisms of P450 cooperativity is that these enzymes can accommodate multiple substrate molecules in one large binding pocket (7-9). It was suggested that the binding of several substrate molecules may be required to promote a productive orientation needed for metabolism. However, recent studies from our and other laboratories suggest that P450 cooperativity represents a true case of allostery involving an effector-induced conformational transition (2,3,10-12), which is thought to modulate the accessibility and degree of hydration of the active site of the enzyme (1,12). In this view pressure perturbation studies of the interactions of CYP3A4 with allosteric ligands are a timely approach to gain further mechanistic insight into active site plasticity as related to allostery.

Perturbation of chemical equilibria by hydrostatic pressure provides a powerful technique for studies of the transitions attributable to changes in hydration of macromolecules, such as protein-protein, protein-DNA, and protein-ligand interactions (13-18). This approach is especially valuable for studies of heme proteins, where the presence of the heme chromophore allows use of various spectroscopic techniques for monitoring the transitions between different states of the enzyme. The first studies of pressure-induced transitions in cytochromes P450 were performed with bacterial P450cam and P450lin (19-24). Later studies utilized mammalian microsomal CYP2B4 (25-27), CYP1A2 (27,28), P450scc (29), and CYP3A4 (11,30), as well as the heme domain of bacterial P450 BM3 (30,31) and cytochrome CYP119 from a thermophilic archaea (32,33).

Application of elevated pressure to ferric cytochromes P450 induces a displacement of the spin equilibrium towards the low spin state (19,22,26,29,31,34). A second barotropic process was identified as the conversion of the P450 into the inactive state known as P420 (22,24-26). In the case of P450cam this P450→P420 transition starts at rather high pressures, when the spin shift is nearly completed (22,35). For other cytochromes P450 these two pressure-induced processes take place in overlapping pressure ranges (23,26,31).

The effect of pressure-induced changes on the content of the high spin form of cytochrome P450 in the presence of substrates reflects two concomitant processes - the dissociation of the enzyme-substrate complex and the changes in the spin equilibrium of both substrate-free and substrate-bound enzyme. Application of advanced methods of spectral analysis to the results of pressure perturbation experiments performed at different substrate concentrations allowed us to resolve the standard volume changes associated with each of these processes in P450cam,

P450 BM3, and CYP2B4 (31). The substrate-free states of all three enzymes exhibited similar values of standard volume change in the low-to-high spin transition (ΔV^{o}_{spin} = +21 − +23 mL/mol), which is consistent with expulsion of one molecule of water per molecule of enzyme. In contrast, the ΔV^{o}_{spin} of the complexes of P450cam, P450 BM3, and CYP2B4 with the substrates camphor, palmitic acid and benzphetamine, respectively, revealed important differences among these enzymes. While in the case of P450 BM3 the value of ΔV^{o}_{spin} remained largely unaltered upon substrate binding, CYP2B4 and P450cam showed a considerable increase in ΔV^{o}_{spin} upon formation of the corresponding substrate complex. Similarly, the enzymes showed important differences in the standard volume changes of the dissociation of the substrate complexes. While increasing hydrostatic pressure caused a dissociation of the complexes of P450cam and P450 BMP with their substrates (ΔV^{o}_{diss} of −48 and −25 mL/mol, respectively), formation of the complex of CYP2B4 with benzphetamine was slightly promoted by pressure (ΔV^{o}_{diss} = 8.1 mL/mol).

The pressure-induced P450→P420 transition in CYP3A4 was characterized in detail in our previous publication (11), where we demonstrated the distribution of the pool of the enzyme in oligomers into two stable fractions (conformers) having different susceptibility to pressure-induced inactivation. The present study is focused on analysis of the effect of substrates on the pressure-induced spin transitions in CYP3A4 in oligomers in solution and in a monomeric state of the enzyme incorporated into Nanodiscs. We show here that, unlike other P450 enzymes studied to date, CYP3A4 both in oligomers in solution and in Nanodiscs exhibits a pressure-dependent equilibrium between two conformational states that differ significantly in the barotropic parameters of spin transitions and substrate binding. We also demonstrate a striking difference in the pressure-induced transitions in CYP3A4 observed with the allosteric substrates testosterone and 1-pyrenebutanol (1-PB) as opposed to the non-allosteric substrate bromocriptine. Our observations are consistent with a large-scale conformational transition in CYP3A4, which modifies the dynamics of the protein-bound water involved in spin transitions and substrate binding and is central to the mechanism of the cooperativity observed in this enzyme.

Materials and methods

Materials

Bromocriptine (BCT) mesylate, 2-hydroxypropyl-β-cyclodextrin (HPCD), and water-soluble testosterone (HPCD-encapsulated testosterone) were the products of Sigma Chemicals (St. Louis, MO). 1-Pyrenebutanol (1-PB) and 4-(dicyanovinyl)julolidine (DCVJ) were from Invitrogen/Molecular Probes Inc. (Eugene, CA). All other chemicals were of ACS grade and were used without further purification.

Expression and purification of CYP3A4

Wild-type CYP3A4 was expressed as a His-tagged protein in *Escherichia coli* TOPP3 cells and purified as described earlier (2).

Preparation of Nanodiscs containing CYP3A4

Soluble nanoscale membrane bilayer particles (Nanodiscs) containing CYP3A4 were obtained by a detergent-removal technique from the mixture of CYP3A4, phospholipid, and a membrane scaffold protein (MSP1D1) as previously described (36). Control experiments showed that the Nanodiscs were stable at hydrostatic pressures up to 4.8 kbar (see Supporting Information to this article).

Experimental

High-pressure spectroscopic studies were performed using a rapid scanning multi-channel MC2000−2 spectrophotometer (Ocean Optics, Inc., Dunedin, FL) equipped with an L7893 UV-VIS fiber light source (Hamamatsu Photonics K.K., Japan). The instrument was connected by a flexible optic cable to the high-pressure cell (20) connected to a manual pressure generator capable of generating a pressure of 6000 bar. All experiments were carried out at 25 °C in 100 mM Na-HEPES buffer, pH 7.4, containing 1 mM DTT and 1 mM EDTA. This buffer is known to be appropriate for pressure-perturbation experiments, as it exhibits a pressure-induced pH change of only −0.06 pH units per kilobar (25).

BCT was used in the form of 300 μM solution in 20 mM Na-acetate buffer, pH 4.0. Control measurements showed that the change in the pH of our samples due to addition of an acidic solution of BCT did not exceed 0.1 pH unit.

1-PB and testosterone were used as complexes with HPCD in order to diminish pressure-induced changes in solubility of these hydrophobic substances. A stock solution of the HPCD complex of 1-PB was prepared on a vortex mixer by mixing 1 volume of a 10 mM acetone solution of 1-PB with 2 volumes of a 30 mg/mL solution of HPCD in 0.1 M Na-Hepes buffer, pH 7.4. A 2.5 mM stock solution of the HPCD-complex of testosterone in the above buffer was prepared using commercially available HPCD-encapsulated testosterone. Control studies presented in Supporting Information showed that replacement of the stock solutions of 1-PB and testosterone in acetone with their water-soluble complexes with HPCD has virtually no effect on the parameters of the interactions of these substrates with CYP3A4 (Fig. S4). Therefore, although increase in hydrostatic pressure results in gradual dissociation of the HPCD complexes (Fig. S5), this process is not expected to have any appreciable effect on the barotropic behavior of the enzyme.

Data Processing

To interpret the experiments in terms of pressure-induced changes in concentration of P450 and P420 we used principal component analysis (PCA) as described earlier (26,37). This approach allowed us to increase significantly the signal-to-noise ratio and to remove the spectral perturbations due to the changes in turbidity of the system during the experiments. To interpret the pressure-induced transitions in terms of changes in concentration of P450 species, we used a least-squares fitting of the spectra of principal components to the set of the spectral standards of pure high-spin P450, low-spin P450, and P420 species of the heme protein (11, 38). Prior to the analysis all spectra were corrected for the compression of the solvent, as described (25).

Our interpretation of the pressure-induced changes is based on the equation for the pressure dependence of the equilibrium constant ((39), eq. 1):

$$\partial\left(\ln \quad K_{eq}\right)/\partial p = -\left(\Delta V^{0}\right)/RT \tag{1}$$

or (in integral form, (40), p. 212, eq.9):

$$K_{eq}=K_{eq}^{0}\cdot e^{-P\Delta V^{0}/RT}=e^{\left(P_{\frac{1}{2}}-P\right)\Delta V^{0}/RT} \tag{2}$$

Here K_{eq} is the equilibrium constants of the reaction at pressure P, $P_{½}$ is the pressure at which $K_{eq} = 1$ (“half pressure” of the conversion), ΔV^{o} is the standard molar reaction volume, and K^{o}_{eq} is the equilibrium constant extrapolated to zero pressure, $K^{o}_{eq} = e^{P_{½}\Delta Vo/RT}$. For the equilibrium A ⇌ B and K^{o}_{eq} =[B]/[A] equation (2) produces the following relationship:

$$[A] = \frac{C_0}{1 + K_{eq}^0 \cdot e^{-P\Delta V^0 / RT}} = \frac{C_0}{1 + e^{\left(P_{\frac{1}{2}} - P\right)\Delta V^0 / RT}} \quad (3)$$

where C_0=[A]+[B]. Curve fitting was performed using our SPECTRALAB software package (26).

Results

Pressure-induced transitions in CYP3A4 incorporated into Nanodiscs

As shown in our previous publication, application of elevated hydrostatic pressure to oligomeric CYP3A4 in solution results in a reversible high-to-low shift of the spin equilibrium, which is followed by a P450→P420 transition. This apparent inactivation process involves no more than 72 ± 6% of the heme protein and is slowly reversible upon decompression (11). In addition to this rapid P450→P420 transition, there was a slower irreversible inactivation process, which takes place upon prolonged incubation of the protein at pressures >1500 bar. This apparent conformational heterogeneity of the protein disappeared upon monomerization of CYP3A4 in the presence of detergent (11). In order to rule out possible involvement of a direct interaction of detergent with CYP3A4 in the above effect we have now studied the pressure-induced transitions of CYP3A4 monomerized by incorporation into lipoprotein Nanodiscs (CYP3A4ND).

Control experiments shown in Supporting Information demonstrated that the tryptophan fluorescence of CYP3A4-containing Nanodiscs exhibits a gradual decrease at increased hydrostatic pressures. This process was completely reversible upon decompression from 4.8 kbar (Fig. S2). Therefore, the pressure-induced changes in the Nanodiscs are reversible, and the elevated pressure does not cause a destruction of their assembly. We also studied the fluorescence of DCVJ as a probe of the microviscosity of the lipid phase (41) to monitor possible pressure-induced changes that might influence CYP3A4 transitions. The results of these control experiments shown in Supporting Information demonstrated that the pressure-induced increase in the viscosity of the lipid phase is completely reversible and is characterized by a ΔV^o of −21 ml/mol and $P_{½}$ = 4.3 kbar (Fig. S3). The small changes in the lipid viscosity below 2.5 kbar, where most of the pressure-induced changes in the spin equilibrium and substrate binding in CYP3A4 are observed, do not seem to affect the barotropic behavior of the enzyme.

The effect of hydrostatic pressure on the absorbance spectra of CYP3A4ND in the presence of a saturating concentration of BCT is illustrated in Fig. 1a along with the changes in the concentrations of the high-spin, low-spin, and P420 states of CYP3A4ND (inset). Although the transitions observed are qualitatively similar to those in CYP3A4 oligomers, the spin shift and P450→P420 transitions are considerably better resolved in CYP3A4ND. The pressure dependencies of the P420 content in CYP3A4ND in the presence of increasing concentrations of BCT are shown in Fig. 1b. In contrast to CYP3A4 oligomers, where only about two-thirds of the total heme protein was susceptible to this process (11), the amplitude of the P450→P420 transition in CYP3A4ND comprises 93 ± 3%, regardless of the substrate concentration. It should be noted that in CYP3A4ND we observed no slow, irreversible P450→P420 conversion of the kind noted with CYP3A4 oligomers (11). The partitioning between P450 and P420 states of CYP3A4ND reaches its steady state in less than 1 minute after pressure increase and reverses completely within 5−10 minutes upon decompression (data not shown). These results are consistent with our initial conclusion that the heterogeneity of P450 in solution in sensitivity to a pressure-induced P450→P420 transition is due to the oligomerization of the enzyme.

CYP3A4ND also differs from the oligomeric enzyme by an increased value of ΔV^{o}_{P420}. In CYP3A4ND the volume change upon P450→P420 transition was as large as −86.9 ± 6.4 mL/mol and revealed no dependence on the substrate concentration, while the value of $P_{½}$ showed a distinct increase upon substrate saturation (Fig. 1). This finding is also in contrast to CYP3A4 oligomers in solution, where ΔV^{o}_{P420} changes from −25 ± 4 to −41 ± 3 mL/mol (11), and the changes in $P_{½}$ were marginal. Therefore, monomerization by incorporation into Nanodiscs stabilizes the enzyme in regard to pressure-induced inactivation by increasing the reaction volume change of the P450→P420 transition. Formation of the CYP3A4ND complex with BCT results in further decrease in the susceptibility of the enzyme to pressure-induced inactivation by increasing the $P_{½}$ of this process.

Analysis of the effect of hydrostatic pressure on the spin equilibrium of CYP3A4 in the presence of increasing concentrations of BCT

While our previous publication and the above data clarify the pressure-induced P450→P420 transition in CYP3A4, the pressure-induced spin shift and the effect of pressure on the affinity of the enzyme for substrates remains to be characterized. To resolve the barotropic parameters of the spin transitions of the substrate-free and BCT-bound CYP3A4 from those of the dissociation of the BCT complex with the enzyme we studied the pressure-induced spin transitions of CYP3A4 in oligomers in solution and CYP3A4ND at a series of BCT concentrations ranging from 0 to 24 μM. In agreement with earlier results (11,42), our ambient pressure titration experiments showed no homotropic cooperativity and a high amplitude of the substrate-induced spin shift in the interactions of this high-affinity substrate with CYP3A4ND (Table 1). As seen from Fig. 2a, addition of BCT increases considerably the amplitude of the pressure-induced spin shift. The same results are presented in Fig. 2b as dependences of the high spin content of CYP3A4ND on BCT concentration (e.g., binding isoterms) at variable pressure.

The curves shown in Fig. 2b may be adequately fitted by the equation for the equilibrium of binary association ((43) eq II-53, page 73) modified to account for a non-zero offset (A_0) and an adjustable coefficient of proportionality between the concentration of the complex and the observed signal (A_{max}) to yield the values of K_D at respective pressures:

$$A([S]_0) = A_0 + A_{max} \cdot ([ES]/[E]_0) = A_0 + A_{max} \cdot \left(\frac{[E]_0 + [S]_0 + K_D - \left\{ ([E]_0 + [S]_0 + K_D)^2 - 4 \cdot [E]_0 \cdot [S]_0 \right\}^{\frac{1}{2}}}{2 \cdot [E]_0} \right) \quad (4)$$

where A($[S]_0$) represent the amplitude of a signal evidencing the substrate binding (high spin fraction of the enzyme in our case) at substrate concentration $[S]_0$.

The equilibrium constants of the spin equilibrium for the substrate-free ($K_{h,free}$) and BCT-bound enzyme ($K_{h,BCT}$) may be found from the high spin content at no substrate added and at saturating BCT given by the A_0 and A_{max} values. The dependencies of the logarithms of $K_{h,free}$, $K_{h,BCT}$ and K_D on pressure shown in Fig. 3a,b exhibit a clear break around 800 − 1000 bar, which is unexpected. Fundamental equations (1) and (2) suggest the pressure dependency of the logarithm of an equilibrium constant to be linear, with a slope determined by the standard reaction volume change in the pressure-induced transition. Observation of a break in these plots suggests that, in addition to the substrate binding and spin equilibria *per se*, CYP3A4ND exhibits an additional pressure-dependent transition affecting the ΔV^{o} values of the above processes. In other words, the enzyme appears to be subjected to a pressure-dependent equilibrium between two distinct states having different barotropic parameters of the spin transitions and BCT binding. We designate these two putative conformational states of the protein as “R” (for “relaxed”) and “P” (for “pressure-promoted”) states and refer to the transition between them as the “R→P transition”.

To determine the barotropic parameters of the R→P transition we plotted the first derivatives of the logarithms of $K_{h,free}$, $K_{h,BCT}$ and K_D versus pressure. As shown in Fig. 3 (right panels) these plots are represented by sigmoidal curves obeying the equation for pressure dependence of the concentration of a compound subjected to an equilibrium transition (eq. 3). The fitting of these curves yields the values of ΔV^o of −69 mL/mol for both constants of spin transitions ($K_{h,free}$ and $K_{h,BCT}$) and −98 mL/mol for the constant of dissociation of substrate complex (K_D).

Similar behavior was also observed in the oligomers of CYP3A4 in solution, where the parameters of the enzyme interactions with BCT at ambient pressure were close to those observed in CYP3A4ND (Table 1). The plots of the high spin content in CYP3A4 versus pressure at different concentrations of BCT are shown in Fig. 4a. The corresponding dependencies of the high spin fraction on BCT concentration at different pressures obey the equation for the equilibrium of binary association (Fig. 4b), and the plots of the logarithms of $K_{H,free}$, $K_{H,BCT}$ and K_D on pressure exhibit distinct breaks in the range of 1000 − 1500 bar (Fig. 5a,b). The break in the plot for ln(K_D) is especially illustrative, as it reflects the change in the sign of ΔV^o, so that an increase in hydrostatic pressure in the low pressure range results in dissociation of the complex, whereas BCT binding is promoted at pressures >1500 bar. Similar to the observations with CYP3A4ND, the plots of the derivatives of the logarithms of the equilibrium constants vs. pressure reveal a pressure-induced transition in CYP3A4 in solution, which changes the values of $\Delta V^o_{H,free}$, $\Delta V^o_{H,BCT}$ and ΔV^o_{diss} (Fig. 5, right panels). The values of ΔV^o of this transition determined from the plots for $K_{H,free}$, $K_{H,BCT}$ and K_D are as large as −50 to −90 mL/mol (Table 2). The remarkable similarity of these results to those reported above for CYP3A4ND suggests that the incorporation of CYP3A4 into Nanodiscs and possible pressure-induced rearrangements in the scaffold protein and/or lipid bilayer have no significant effect on the observed barotropic behavior of the enzyme in Nanodiscs.

Analysis of the effect of hydrostatic pressure on the spin equilibrium of CYP3A4 in Nanodiscs and in solution in the presence of substrates demonstrating homotropic cooperativity

The results presented above reveal a pressure-dependent equilibrium between two states of the enzyme that affects the BCT-induced spin transitions in both CYP3A4ND and CYP3A4 in solution. To probe possible involvement of this apparent conformational transition in the mechanisms of cooperativity of CYP3A4 we studied the effect of hydrostatic pressure on the spin state of CYP3A4 in the presence of various concentrations of testosterone and 1-PB, type I substrates where homotropic cooperativity is observed. The HPCD complexes of the substrates were used to approach saturating concentrations and minimize the effect of pressure-induced changes in solubility. The parameters of the interactions of CYP3A4 with these substrate obtained from the ambient pressure titration experiments are given in Table 1. It should be noted, however, that due to a profound decrease in the affinity for 1-PB observed upon CYP3A4 incorporation into the Nanodiscs (data not shown), the studies of the interactions of CYP3A4ND with this substrate were precluded by its low solubility and high extinction coefficient in the Soret region. Therefore, the studies with the enzyme incorporated into the Nanodiscs were limited to the case of testosterone only.

The pressure-induced changes in CYP3A4ND in the presence of 280 μM testosterone are illustrated in Fig. 6a. Comparison of this figure with the transitions observed in the presence of BCT in CYP3A4 in Nanodiscs (Fig. 1) and in solution ((11), Fig. 3) reveals a critical difference. Namely, the pressure-dependence of the spin state in the presence of testosterone has a considerably lower amplitude than in the complex of the enzyme with BCT. Even at a pressure as high as 4 kbar there is a significant high spin CYP3A4 content in the presence of testosterone. In contrast, both in solution and in Nanodiscs there is no high spin heme protein

above 3 kbar in the absence of substrate or presence of BCT. Similar behavior was also observed for CYP3A4 in solution in the presence of either testosterone (Fig 6b) or 1-PB (Fig. 6c). To rule out possible involvement of substrate interactions with HPCD we also performed a series experiments with CYP3A4 in solution in the presence of 1-PB added as a 15 mM stock solution in acetone with no HPCD present. The behavior of CYP3A4 revealed in these experiments was similar to that shown in Fig. 6c for the complex of 1-PB with HPCD (data not shown).

The difference in the barotropic behavior of CYP3A4 with 1-PB and testosterone as opposed to BCT becomes especially evident from the analysis of the pressure-induced changes in the spin state of CYP3A4 observed at various concentrations of substrate. As one can see from Fig 7a (left panel), although displacing the spin equilibrium towards the high spin state, testosterone does not increase the amplitude of the pressure-induced spin shift to the same extent. Consequently, in contrast to other cytochromes P450 where the amplitude of the substrate-induced spin shift at elevated pressures approaches zero (26,31,39), the substrate-induced spin shift in the interactions of CYP3A4ND with testosterone remains considerable even at pressures above 2000 bar, where no further decrease in the high spin content is observed (Fig. 7a, right panel). A similar phenomenon was observed with CYP3A4 in solution with both testosterone (Fig. 7b) and 1-PB (Fig. 7c). This unusual behavior of CYP3A4 with substrates exhibiting homotropic cooperativity is especially evident in the case of the interactions of CYP3A4 in solution with 1-PB (Fig. 7c, left panel). Importantly, similar barotropic behavior was also observed in preliminary studies on the interactions of CYP3A4 in solution with α-naphthoflavone, another substrate exhibiting homotropic cooperativity (data not shown).

Analysis of the pressure dependence of the constant of spin equilibrium in the complexes of CYP3A4ND and CYP3A4 in solution is illustrated in Fig. 8. In common with observations on the interactions of CYP3A4 with BCT, the non-linear pressure dependencies of $\ln(K_h)$ in the complexes of CYP3A4 with testosterone and 1-PB (Fig. 8a) suggest a pressure-dependent equilibrium between two states of the enzyme characterized by different values of ΔV^o_{spin}. However, in contrast to the substrate-free enzyme and the CYP3A4 complexes with BCT, where this putative R→P transition resulted in an *increase* in the value of ΔV^o_{spin} , the complexes of both CYP3A4 oligomers and CYP3A4ND with allosteric substrates reveal an important *decrease* in ΔV^o_{spin} upon transition to the pressure-promoted conformation. The molar volume change in the spin transition approaches zero upon the conversion of the complexes of CYP3A4 with testosterone and 1-PB into the pressure-promoted state (Table 2).

The analysis of the pressure dependence of substrate binding isotherms shown in the right panels of Fig. 8b,c suggests an important increase in the cooperativity of the interactions at elevated pressures, where the values of the Hill coefficient for the interactions of CYP3A4 in solution with testosterone and 1-PB approach 3.3 and 1.9 respectively (Fig. 9). In both cases this increase in cooperativity was associated with changes in S_{50} values analogous to those shown in Fig. 5b for the K_D of the complex of CYP3A4 with BCT (data not shown). An initial increase in the S_{50} values with increasing pressure is followed by a sharp decrease at pressures >1200 bar. This behavior is also consistent with a pressure-induced conformational transition in the enzyme that changes the sign of the volume changes observed upon substrate dissociation (Table 2). In contrast, no considerable pressure-induced changes in the values of S_{50} and the Hill coefficient for the interactions with testosterone were observed in CYP3A4ND (data not shown). These results suggest that homotropic cooperativity in CYP3A4 represents a true case of allostery that involves transitions between several conformational states of the enzyme characterized by different values of ΔV^o_{spin} and $\Delta V^o_{diss.}$ Interactions of the enzyme with the allosteric substrates appears to induce a conformational transition that decreases water accessibility and/or degree of hydration of the active site, so that water flux into the heme pocket is impeded and the high-spin state of the heme iron is stabilized.

Discussion

Our pressure-perturbation experiments on CYP3A4-substrate interactions using enzyme in solution and in Nanodiscs have yielded three pivotal findings that have broad implications for an understanding of cytochrome P450 function and cooperativity. First, with both kinds of CYP3A4 preparations there are some striking differences between this allosteric enzyme and the other cytochromes P450 studied previously in several laboratories. Second, the barotropic behavior of CYP3A4 differs dramatically in the presence of the allosteric substrates testosterone and 1-PB as opposed to the non-allosteric substrate BCT, Third, differences between the behavior of oligomeric CYP3A4 in solution compared with monomeric enzyme in Nanodiscs confirm and extend our previous findings on the existence of stable, functionally distinct conformers in the oligomers. Overall, pressure-perturbation spectroscopy promises to be an invaluable complement to other approaches our laboratory has introduced recently to analyze mechanisms of CYP3A4 cooperativity (1,2,38).

In contrast to CYP2B4, P450cam, and P450 BMP, which exhibit no apparent changes in $\Delta V^{o}_{H,free}$, $\Delta V^{o}_{H,S}$ and ΔV^{o}_{diss} with pressure, CYP3A4 revealed a pressure-induced transition that changes the values of ΔV^{o} of the substrate dissociation and spin transitions. This important difference between CYP3A4 and other P450 heme proteins studied to date is especially evident upon comparison of Fig. 3, Fig. 5, and Fig. 8 with Fig. 10, which shows similar plots for the heme domain of cytochrome P450 BM3 (BMP) based on our earlier results (31).

Four states of the P450 are routinely considered in the analysis of substrate- and pressure-induced spin transitions (26,31,39), namely the low- and high spin states of both the substrate free and substrate-bound enzyme. Our studies reveal an additional pressure-sensitive equilibrium between two distinct conformational states of CYP3A4, designated here as “R” (for “relaxed”) and “P” (for “pressure-promoted”) states. The pressure-induced transition between these states causes a non-linearity of the plots of the logarithms of the apparent values of $K_{H,free}$, $K_{H,S}$, and K_D versus pressure. It is important to note that the non-linearity of the plots is observed in oligomeric CYP3A4 in solution (Fig. 5, Fig. 8b,c) as well as monomeric CYP3A4ND (Fig. 3, Fig. 8a), suggesting that this apparent pressure-sensitive conformational equilibrium constitutes an inherent feature of the CYP3A4 monomer.

The slope of the plots of the logarithms of the constants of equilibrium versus pressure is therefore determined by the partitioning between the R- and P-states at each given pressure, so that the dependencies of $-d(ln(K_{eq})\times RT))/d(P)$ on pressure reflect the changes in the fraction of the pressure-promoted P-state. Fitting of these derivative plots (Fig. 3, Fig. 5, and Fig. 8, right panels) to eq. 3 allows us to determine the barotropic parameters of the transition between these two conformations of the enzyme (Table 2). As CYP3A4ND and the enzyme in solution both revealed a considerable negative volume change (−45 to −98 mL/mol) in the R→P transition in both substrate-free enzyme and in the complexes with BCT, testosterone and 1-PB, this transition is likely to involve an important increase in the protein hydration.

The most striking observation in this study is that the enzyme saturated with testosterone or 1-PB becomes refractory to pressure-induced displacement of spin and substrate binding equilibria upon the transition to the P-state (at pressures >1600 bar). Insight into the mechanistic basis of this unusual behavior becomes possible upon the analysis of the plots of the derivatives of $ln(K_h)$ and $ln(S_{50})$ versus pressure. The limits that these plots approach at infinitely increasing or decreasing pressure provide us with estimates of the corresponding ΔV^{o} values for the P- and R-states, respectively. Analysis of these values (Table 2) reveals an important difference between the substrate-free or BCT-bound enzyme and the complexes of CYP3A4 with testosterone or 1-PB. In contrast to the substrate-free or BCT-bound enzyme, where the R→P transition results in a considerable increase in the positive value of ΔV^{o}_{spin} (Table 2),

the R→P transition of the complexes of the enzyme with allosteric substrates causes a decrease in ΔV^{o}_{spin} to zero or even negative values, as in the complex of CYP3A4ND with testosterone (Table 2). This difference in the mechanisms of interactions is also revealed in the values of ΔV^{o}_{diss}. Whereas the dissociation of the BCT complexes of the R-state of either CYP3A4 in solution or CYP3A4ND is associated with an important negative volume change (−74 and −31 mL/mol respectively), the value of ΔV^{o}_{diss} of the complexes of the R-state of CYP3A4 with allosteric substrates is as low as −15 or −7 mL/mol (in the complexes of CYP3A4 in solution with testosterone or 1-PB respectively) or even equal to 0, as in the case of the complex of CYP3A4ND with testosterone. Furthermore, in the case of CYP3A4 in solution the R→P transition results in a change in the sign of ΔV^{o}_{diss} of the complexes with testosterone and 1-PB (Table 2). Due to such non-negative values of ΔV^{o}_{diss} in the pressure-promoted state, elevated hydrostatic pressure is incapable of causing complete dissociation of the complexes of CYP3A4ND or CYP3A4 oligomers with allosteric substrates. This observation coupled with the above finding that the values of ΔV^{o}_{spin} of these complexes approaches zero or even changes sign upon the transition to the P-state (Table 2) explains why elevated pressure cannot displace the spin equilibrium in these complexes completely to the low-spin state.

The observation that elevated hydrostatic pressure induces an important increase in the cooperativity of CYP3A4 in solution with either testosterone or 1-PB (Fig. 9) suggests a tight connection between the R↔P conformational equilibrium and the mechanisms of cooperativity. Interestingly, the dependencies of the Hill coefficient on pressure fit adequately to eq. 3 for pressure dependency of equilibrium (Fig 9, solid lines), with the ΔV^{o} values of −56 and −69 mL/mol for the cases of testosterone and 1-PB respectively, which are consistent with the values for the R↔P transition derived from the analysis of the derivative plots (Table 2). Involvement of the R→P transition in the mechanisms of cooperativity is also revealed in a displacement of the conformational equilibrium towards the P-state by testosterone observed in both CYP3A4 in solution and CYP3A4ND (Table 2).

Accordingly, our results suggest that the mechanisms of cooperativity in CYP3A4 involve a complex system of transitions in an ensemble of conformational states differing in the degree of hydration and water accessibility of the heme pocket. Although we are far from a detailed understanding of the conformational dynamics of the enzyme involved in the allosteric mechanisms, our results led us to the following basic assertions. In the absence of substrate the enzyme is represented by two conformational states (R- and P-states) differing in the ΔV^{o} of spin transition and substrate binding. The transition from the R to P state requires an important hydration of the protein so that the equilibrium between these states is displaced towards the P-state by hydrostatic pressure. The binding of a non-allosteric substrate (BCT) to the R-state is associated with a large positive volume change, whereas the volume changes upon the formation of the complexes of this state with allosteric substrates are considerably lower. That may indicate that the binding of the first (effector) molecule of these substrates, which is silent in terms of substrate-induced spin shift, causes a conformational transition that facilitates the binding of the second substrate molecule. Although distinct from the R→P transition, this effector-induced rearrangement is able to displace the conformational equilibrium towards the P-state, as seen in the case of CYP3A4 interactions with testosterone (Table 2). The fact that the saturation of the enzyme with testosterone and 1-PB abolishes the effect of hydrostatic pressure on substrate binding and spin equilibrium in the P-state suggests that the interactions of this conformer of the enzyme with allosteric substrates results in a drastic decrease in hydration and/or water accessibility of the heme pocket. It should be noted that, although the conformational equilibrium in CYP3A4 in solution and in CYP3A4ND is largely shifted towards the R-state, a different situation may take place in the microsomal membrane, where the conformational equilibrium may be displaced by the interactions of CYP3A4 with NADPH-cytochrome P450 reductase and/or cytochrome b_5. This suggestion is consistent with our earlier observation that the barotropic behavior of the recombinant CYP3A4 in the

membranes of yeast microsomes is similar to that reported here for the complexes of the P state of CYP3A4 with allosteric substrates in that hydrostatic pressure was unable to displace the spin equilibrium of the substrate-free or BCT-saturated enzyme completely to the low-spin state (11).

In addition to discovery of a pressure-sensitive conformational equilibrium, the data obtained with the monomeric CYP3A4ND confirm our earlier conclusion that the persistent conformational heterogeneity observed in CYP3A4 in solution (1,11) is due to the oligomerization of the enzyme. The change from oligomers of CYP3A4 in solution to the monomeric enzyme in Nanodiscs virtually abolishes this heterogeneity, as reflected in the pressure-induced P450→P420 transition. Previously we showed that the incorporation of the enzyme into Nanodiscs results in a disappearance of the middle phase of the three-exponential reduction kinetics with dithionite observed in oligomers (1). The relationship between the newly discovered pressure-sensitive conformational equilibrium in CYP3A4 with the persistent conformational heterogeneity of the enzyme in oligomers, which appears to be unaffected by pressure, remains unclear. An intriguing possibility is that the fraction of CYP3A4 in oligomers that is refractory to a pressure induced P450→P420 transition and is represented in the middle phase of the dithionite-dependent reduction may be excluded from the newly-discovered R↔P equilibrium.

In summary, this study shows that pressure-perturbation experiments on CYP3A4-substrate interactions provide a valuable tool for the exploration of cooperativity. The involvement of the large-range conformational transitions of CYP3A4 in the allosteric mechanisms demonstrated in this study is consistent with high conformational mobility of CYP3A4, as evidenced by recently resolved X-ray structures of the enzyme with erythromycin or ketoconazole (6). We believe that further studies combining the static pressure perturbation or pressure-jump techniques with methods capable of detecting conformational transitions, such as fluorometric spectroscopy with the enzyme labeled with appropriate probes, NMR, or FT-IR spectroscopy, will provide a key for deeper understanding of the involvement of conformational malleability of CYP3A4 in the allosteric mechanisms.

Supplementary Material

Refer to Web version on PubMed Central for supplementary material.

Acknowledgements

The authors are grateful to Dr. Yelena V. Grinkova and Dr. Ilia G. Denisov (Department of Biochemistry, University of Illinois at Urbana-Champaign) for their help in the studies with Nanodiscs.

Abbreviations and textual footnotes

CYP3A4, cytochrome P450 3A4; Hepes, N-[2-hydroxyethylpiperazine-N'-[2-ethanesulfonic acid]; DTT, dithiothreitol; EDTA, ethylenediaminetetraacetic acid; CYP3A4ND, CYP3A4 incorporated into Nanodiscs; BCT, bromocriptine; 1-PB, 1-pyrenebutanol; HPCD, 2-hydroxypropyl-β-cyclodextrin; DCVJ, 4-(dicyanovinyl)julolidine..

References

1. Davydov DR, Fernando H, Baas BJ, Sligar SG, Halpert JR. Kinetics of dithionite-dependent reduction of cytochrome P450 3A4: Heterogeneity of the enzyme caused by its oligomerization. Biochemistry 2005;44:13902–13913. [PubMed: 16229479]

2. Tsalkova TN, Davydova NE, Halpert JR, Davydov DR. Mechanism of interactions of alpha-naphthoflavone with cytochrome P450 3A4 explored with an engineered enzyme bearing a fluorescent probe. Biochemistry 2007;46
3. Lampe JN, Atkins WM. Time-resolved fluorescence studies of heterotropic ligand binding to cytochrome P450 3A4. Biochemistry 2006;45:12204–12215. [PubMed: 17014074]
4. Scott EE, White MA, He YA, Johnson EF, Stout CD, Halpert JR. Structure of mammalian cytochrome P450 2B4 complexed with 4-(4-chlorophenyl)imidazole at 1.9-A resolution: insight into the range of P450 conformations and the coordination of redox partner binding. J. Biol. Chem 2004;279:27294–27301. [PubMed: 15100217]
5. Zhao Y, White MA, Muralidhara BK, Sun L, Halpert JR, Stout CD. Structure of microsomal cytochrome P450 2B4 complexed with the antifungal drug bifonazole: insight into P450 conformational plasticity and membrane interaction. J. Biol. Chem 2006;281:5973–5981. [PubMed: 16373351]
6. Ekroos M, Sjögren T. Structural basis for ligand promiscuity in cytochrome P450 3A4. Proc. Natl. Acad. Sci. U. S. A 2006;103:13684–13687.
7. Shou M, Grogan J, Mancewicz JA, Krausz KW, Gonzalez FJ, Gelboin HV, Korzekwa KR. Activation of CYP3A4 - evidence for the simultaneous binding of 2 substrates. Biochemistry 1994;33:6450–6455. [PubMed: 8204577]
8. Korzekwa KR, Krishnamachary N, Shou M, Ogai A, Parise RA, Rettie AE, Gonzalez FJ, Tracy TS. Evaluation of atypical cytochrome P450 kinetics with two-substrate models: evidence that multiple substrates can simultaneously bind to cytochrome P450 active sites. Biochemistry 1998;37:4137–4147. [PubMed: 9521735]
9. Ueng YF, Kuwabara T, Chun YJ, Guengerich FP. Cooperativity in oxidations catalyzed by cytochrome P450 3A4. Biochemistry 1997;36:370–381. [PubMed: 9003190]
10. Atkins WM, Wang RW, Lu AYH. Allosteric behavior in cytochrome P450-dependent in vitro drug-drug interactions: A prospective based on conformational dynamics. Chem. Res. Toxicol 2001;14:338–347. [PubMed: 11304120]
11. Davydov DR, Halpert JR, Renaud JP, Hui Bon Hoa G. Conformational heterogeneity of cytochrome P450 3A4 revealed by high pressure spectroscopy. Biochem. Biophys. Res. Commun 2003;312:121–130. [PubMed: 14630029]
12. Davydov DR, Botchkareva AE, Kumar S, He YQ, Halpert JR. An electrostatically driven conformational transition is involved in the mechanisms of substrate binding and cooperativity in cytochrome P450eryF. Biochemistry 2004;43:6475–6485. [PubMed: 15157081]
13. Li H, Akasaka K. Conformational fluctuations of proteins revealed by variable pressure NMR. Biochim Biophys Acta 2006;1764:331–345. [PubMed: 16448868]
14. Occhipinti E, Bec N, Gambirasio B, Baietta G, Martelli PL, Casadio R, Balny C, Lange R, Tortora P. Pressure and temperature as tools for investigating the role of individual non-covalent interactions in enzymatic reactions Sulfolobus solfataricus carboxypeptidase as a model enzyme. Biochim. Biophys. Acta 2006;1764:563–572. [PubMed: 16446132]
15. Kornblatt JA, Kornblatt MJ. The effects of osmotic and hydrostatic pressures on macromolecular systems. Biochim. Biophys. Acta 2002;1595:30–47. [PubMed: 11983385]
16. Macgregor RB. The interactions of nucleic acids at elevated hydrostatic pressure. Biochim. Biophys. Acta 2002;1595:266–276. [PubMed: 11983401]
17. Heremans K, Smeller L. Protein structure and dynamics at high pressure. Biochim. Biophys. Acta 1998;1386:353–370. [PubMed: 9733996]
18. Robinson CR, Sligar SG. Hydrostatic pressure reverses osmotic pressure effects on the specificity of EcoRI-DNA interactions. Biochemistry 1994;33:3787–3792. [PubMed: 8142380]
19. Fisher MT, Scarlata SF, Sligar SG. High-pressure investigations of cytochrome P-450 spin and substrate binding equilibria. Arch. Biochem. Biophys 1985;1:456–463. [PubMed: 2990349]
20. Hui Bon Hoa G, Marden MC. The pressure dependence of the spin equilibrium in camphor-bound ferric cytochrome P-450. Eur. J. Biochem 1982;124:311–315. [PubMed: 6284506]
21. Marden MC, Hoa GH. P-450 binding to substrates camphor and linalool versus pressure. Arch. Biochem. Biophys 1987;253:100–107. [PubMed: 3813557]

22. Di Primo C, Hui Bon Hoa G, Douzou P, Sligar SG. Heme-pocket-hydration change during the inactivation of cytochrome P-450camphor by hydrostatic pressure. Eur. J. Biochem 1992;2:583–508. [PubMed: 1425665]
23. Hui Bon Hoa G, Di Primo C, Dondaine I, Sligar SG, Gunsalus IC, Douzou P. Conformational changes of cytochromes P-450cam and P-450lin induced by high pressure. Biochemistry 1989;28:651–656. [PubMed: 2578028]
24. Tschirret-Guth RA, Hui Bon Hoa G, Ortiz de Montellano RP. Pressure-induced deformation of the cytochrome P450cam active site. J. Am. Chem. Soc 1998;120:3590–3596.
25. Davydov DR, Knyushko TV, Hui Bon Hoa G. High pressure induced inactivation of ferrous cytochrome P-450 LM2 (2B4) CO complex: evidence for the presence of two conformers in the oligomer. Biochem .Biophys.Res.Commun 1992;188:216–221. [PubMed: 1417844]
26. Davydov DR, Deprez E, Hui Bon Hoa G, Knyushko TV, Kuznetsova GP, Koen YM, Archakov AI. High-pressure induced transitions in microsomal cytochrome P450 2B4 in solution - evidence for conformational Inhomogeneity in the oligomers. Arch. Biochem. Biophys 1995;320:330–344. [PubMed: 7625841]
27. Davydov DR, Petushkova NA, Archakov AI, Hui Bon Hoa G. Stabilization of P450 2B4 by its association with P450 1A2 revealed by high-pressure spectroscopy. Biochem. Biophys. Res. Commun 2000;276:1005–1012. [PubMed: 11027582]
28. Anzenbacher P, Bec N, Hudecek J, Lange R, Anzenbacherova E. High conformational stability of cytochrome P-450 1A2. Evidence from UV absorption spectra. Collect. Czech. Chem. Commun 1998;63:441–448.
29. Bancel F, Bec N, Ebel C, Lange R. A central role for water in the control of the spin state of cytochrome P-450(scc). Eur. J. Biochem 1997;250:276–285. [PubMed: 9428674]
30. Anzenbacherova E, Bec N, Anzenbacher P, Hudecek J, Soucek P, Jung C, Munro AW, Lange R. Flexibility and stability of the structure of cytochromes P450 3A4 and BM-3. Eur. J. Biochem 2000;267:2916–2920. [PubMed: 10806389]
31. Davydov DR, Hui Bon Hoa G, Peterson JA. Dynamics of protein-bound water in the heme domain of P450BM3 studied by high-pressure spectroscopy: Comparison with P450cam and P450 2B4. Biochemistry 1999;38:751–761. [PubMed: 9888815]
32. Mclean MA, Maves SA, Weiss KE, Krepich S, Sligar SG. Characterization of a cytochrome P450 from the acidothermophilic archaea Sulfolobus solfataricus. Biochem. Biophys. Res. Commun 1998;252:166–172. [PubMed: 9813164]
33. Tschirret-Guth RA, Koo LS, Hoa GHB, de Montellano PRO. Reversible pressure deformation of a thermophilic cytochrome P450 enzyme (CYP119) and its active-site mutants. J. Am. Chem. Soc 2001;123:3412–3417. [PubMed: 11472111]
34. Di Primo C, Deprez E, Hui Bon Hoa G, Douzou P. Antagonistic effects of hydrostatic pressure and osmotic pressure on cytochrome P-450(cam) spin transition. Biophys J 1995;68:2056–2061. [PubMed: 7612848]
35. Di Primo C, Hui Bon Hoa G, Douzou P, Sligar S. Effect of the tyrosine 96 hydrogen bond on the inactivation of cytochrome P-450cam induced by hydrostatic pressure. Eur. J. Biochem 1990;193:383–386. [PubMed: 2226459]
36. Baas BJ, Denisov IG, Sligar SG. Homotropic cooperativity of monomeric cytochrome P450 3A4 in a nanoscale native bilayer environment. Arch. Biochem. Biophys 2004;430:218–228. [PubMed: 15369821]
37. Renaud JP, Davydov DR, Heirwegh KPM, Mansuy D, Hui Bon Hoa G. Thermodynamic studies of substrate binding and spin transitions in human cytochrome P450 3A4 expressed in yeast microsomes. Biochem. J 1996;319:675–681. [PubMed: 8920966]
38. Fernando H, Halpert JR, Davydov DR. Resolution of multiple substrate binding sites in cytochrome P450 3A4: the stoichiometry of the enzyme-substrate complexes probed by FRET and Job's titration. Biochemistry 2006;45:4199–4209. [PubMed: 16566594]
39. Hui Bon Hoa G, McLean MA, Sligar SG. High pressure, a tool for exploring heme protein active sites. Biochim. Biophys. Acta 2002;1595:297–308. [PubMed: 11983404]
40. Weber, G. Protein Interactions. Chapman and Hall; New York: 1991.

41. Kung CE, Reed JK. Microviscosity measurements of phospholipid bilayers using fluorescent dyes that undergo torsional relaxation. Biochemistry 1986;25:6114–6121.

42. Denisov IG, Baas BJ, Grinkova YV, Sligar SG. Cooperativity in P450 CYP3A4: linkages in substrate binding, spin state, uncoupling and product formation. J. Biol. Chem 2007;282:7066–7076. [PubMed: 17213193]

43. Segel, IH. Enzyme Kinetics: Behavior and Analysis of Rapid Equilibrium and Steady-State Enzyme Systems. Wiley-Interscience; New York: 1975.

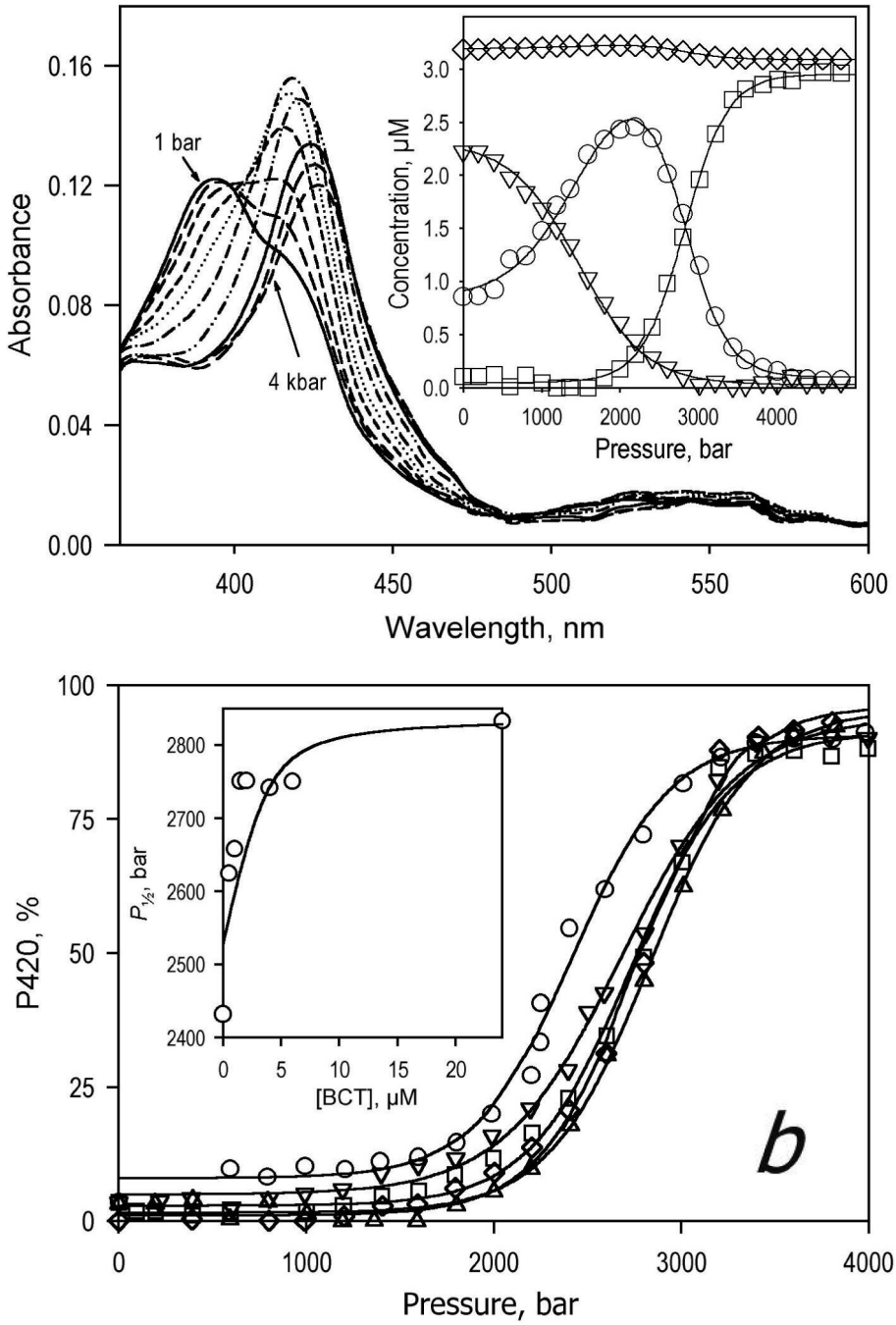

Fig. 1.

Pressure-induced transitions in CYP3A4 in Nanodiscs in the presence of BCT. ***a:*** A series of spectra in the presence of 24 μM BCT recorded at 1 bar (solid line), 800 bar (long dash), 1200 bar (medium dash), 1600 bar (short dash), 2000 bar (dots), 2400 bar (dash-dot), 2800 bar (dash-dot-dot), 3200 bar (solid line), 3600 bar (long dash), and 4000 bar (medium dash). Conditions: 3.2 μM CYP3A4ND in 0.1 M Na-HEPES buffer, pH 7.4, 1mM DTT, 1 mM EDTA, 25°C, optical path length of 0.5 mm. The inset shows the corresponding changes in the concentration of the high-spin (triangles), low-spin (circles), P420 (squares) states of CYP3A4 and the total hemoprotein concentration (diamonds). Panel ***b*** illustrates the course of the pressure-induced P450→P420 transition with no substrate added (circles), and at 0.5 (triangles), 1.5 (squares),

2 (diamonds) and 24 μM BCT (inverted triangles). Solid lines represent the results of fitting of these curves to eq. 3. The inset to this figure shows the dependence of $P_{½}$ found by this fitting on BCT concentration. The corresponding ΔV^{o} values were in the range of 84 − 94 mL/mol and showed no systematic trend with BCT concentration.

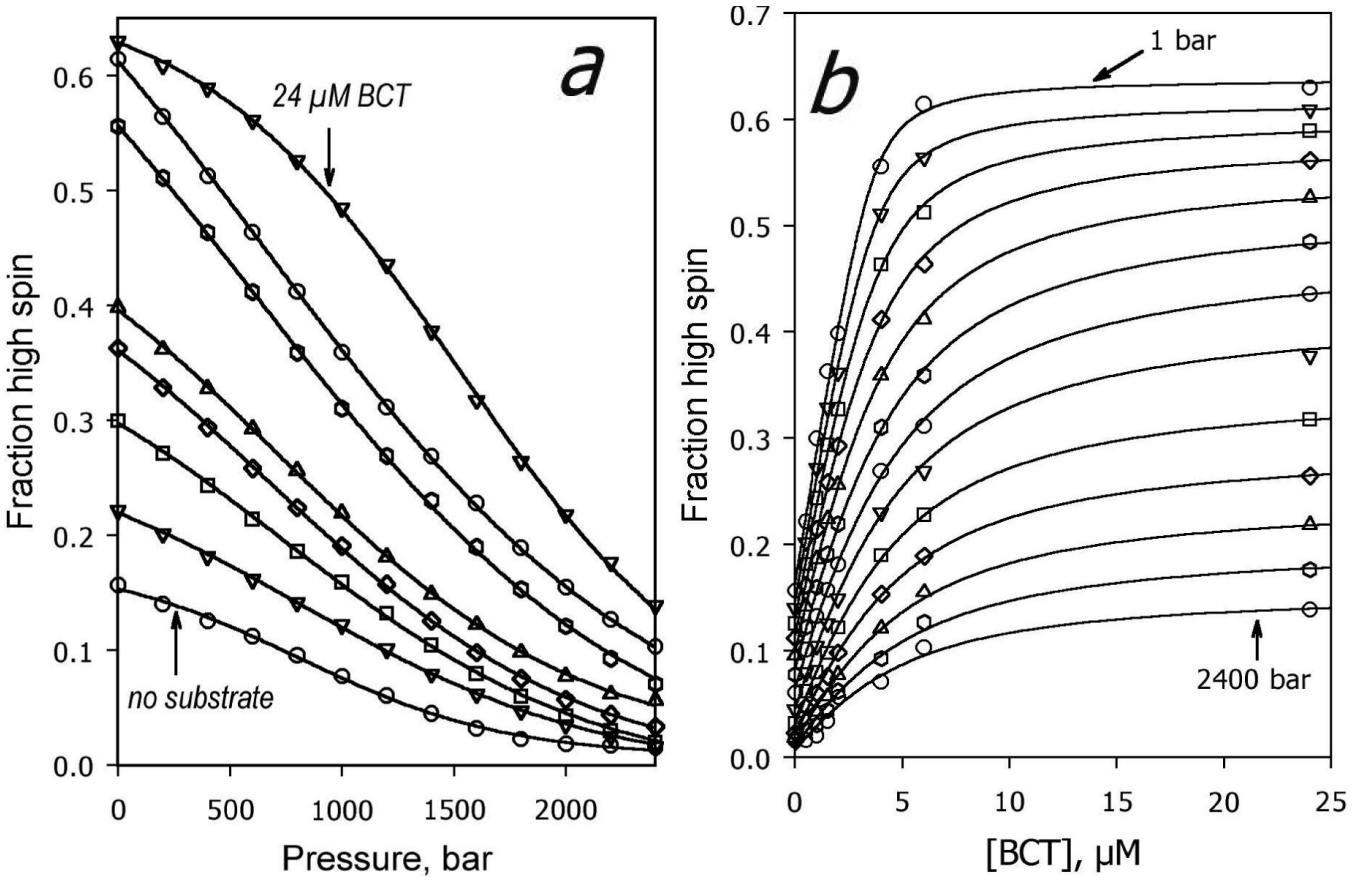

Fig. 2.

Effect of hydrostatic pressure on the spin state of CYP3A4 in Nanodiscs at increasing concentrations of bromocriptine. Panel ***a*** shows the dependencies of the high spin content in CYP3A4ND on pressure at no substrate added (circles), 0.5 (triangles), 1 (squares), 1.5 (diamonds), 2 (inverted triangles), 4 (hexagons), 6 (circles) and 24 μM BCT (triangles). Solid lines represent the results of fitting of these curves to eq. 3. Panel ***b*** shows the same data set as the dependencies of the high spin content on the substrate concentration at a series of hydrostatic pressures increasing from 1 bar to 2400 bar in 200 bar increments. Solid lines show the results of fitting of the titration curves by eq. 4. Conditions as indicated in Fig. 1.

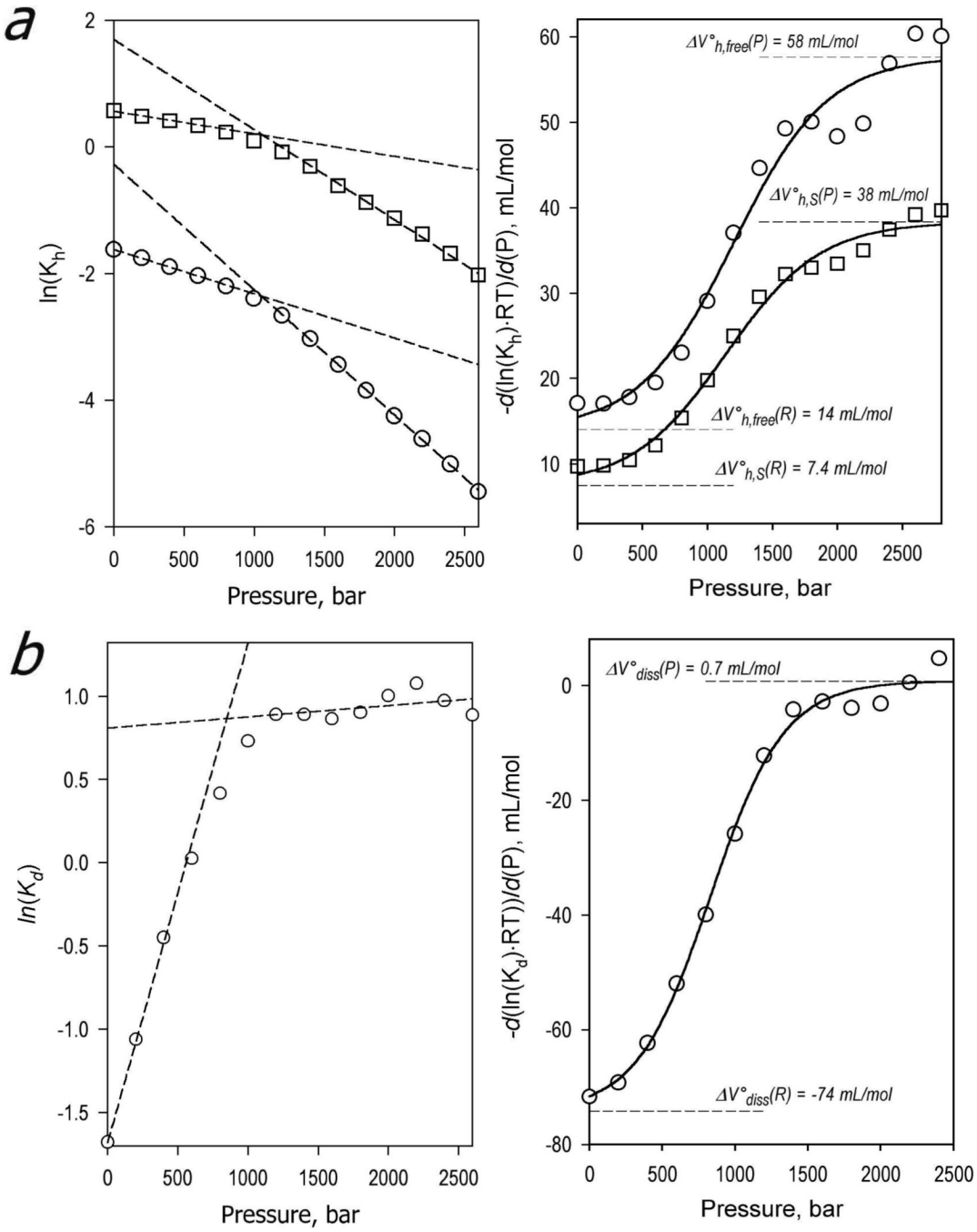

Fig.3.

Effect of hydrostatic pressure on the parameters of spin equilibrium and BCT binding in CYP3A4ND. Panels ***a*** illustrate the effect of hydrostatic pressure on the constant of spin equilibrium of the substrate-free (circles) and BCT-bound enzyme (squares). Panels ***b*** exemplify the pressure dependence of the dissociation constant of the BCT complex of the enzyme. Left panels show the pressure dependencies of the logarithms of the respective constants, whereas the right panels represent the first derivatives of the above dependencies approximated by a 5-th order polynomial. Dashed lines shown in the left panels show a linear approximation of the initial and final parts of the curves. Solid lines shown in the right panels represent the results of fitting of the respective data sets by eq. 3 with the parameters

characterized in Table 2. The low- and high-pressure limits of the respective fitting curves shown in the right panels give the ΔV^{o} values that characterize the putative “R” and “P” conformational states of the enzyme, respectively.

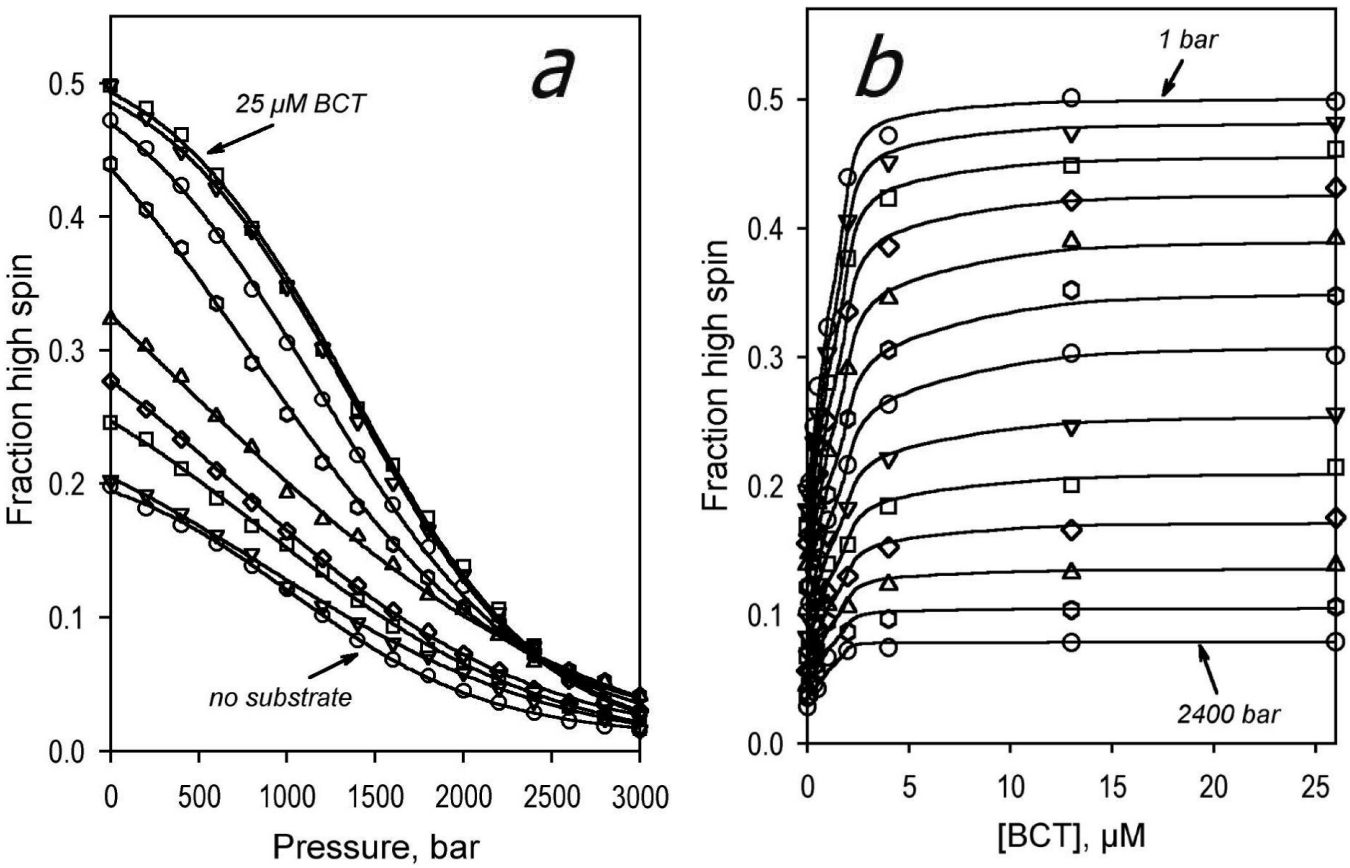

Fig. 4.

Effect of hydrostatic pressure on the spin state of CYP3A4 in solution at increasing concentrations of BCT. Panel ***a*** shows the dependencies of the high spin content on pressure at no substrate added (circles), 0.1 (triangles), 0.35 (squares), 0.5 (diamonds), 1.0 (inverted triangles), 2.0 (hexagons), 4.0 (circles), 13 (triangles) and 24 μM BCT (squares). Solid lines represent the results of fitting of these curves to eq. 3. Panel ***b*** shows the same data set as the dependencies of the high spin content on the substrate concentration at a series of hydrostatic pressures increasing from 1 bar to 2400 bar in 200 bar increments. Solid lines show the results of fitting of the titration curves by eq. 4. Conditions as indicated in Fig. 1, except for the concentration of CYP3A4, which was equal to 2 μM.

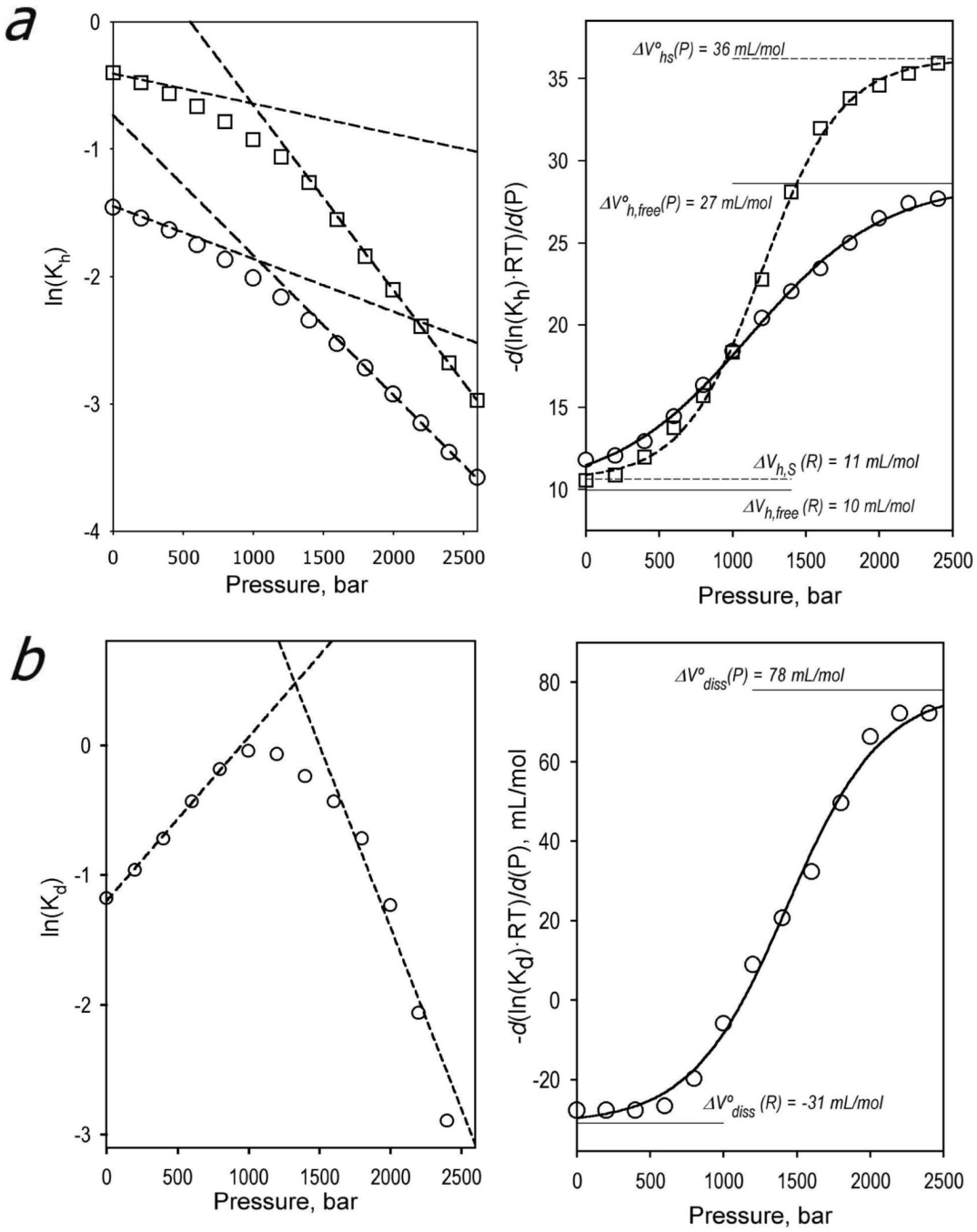

Fig.5.

Effect of hydrostatic pressure on the parameters of spin transitions and dissociation of the complex of CYP3A4 in solution with BCT. The designation of the panels and the keys are similar to those specified for Figure 3.

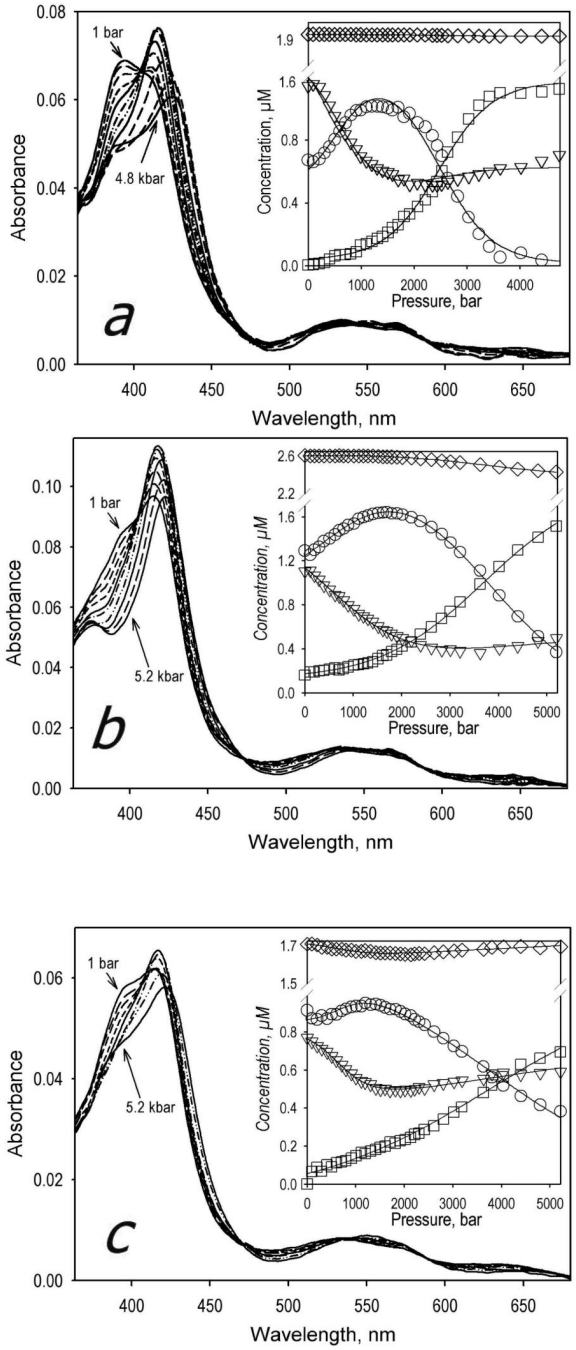

Fig. 6.

Pressure-induced transitions in CYP3A4 in the presence of testosterone and 1-PB. ***a:*** A series of spectra of CYP3A4-ND in the presence of 280 μM testosterone obtained at 1 bar (solid line), 300 bar (long dash), 400 bar (medium dash), 600 bar (short dash), 800 bar (solid line), 1200 bar (dash-dot), 1600 bar (dash-dot-dot), 2000 bar (solid line), 2800 bar (long dash), 3600 bar (medium dash), and 4800 bar (solid line). ***b:*** A series of spectra of CYP3A4 oligomers in solution in the presence of 420 μM testosterone obtained at 1 bar (solid line), 200 bar (long dash), 400 bar (medium dash), 800 bar (short dash), 1200 bar (solid line), 2000 bar (dash-dot), 3600 bar (dash-dot-dot), and 5200 bar (solid line). ***c:*** A series of spectra of CYP3A4 oligomers in solution in the presence of 16 μM 1-PB obtained at 1 bar (solid line), 400 bar (long dash),

800 bar (medium dash), 1200 bar (short dash), 1600 bar (solid line), 2000 bar (dash-dot), 2800 bar (dash-dot-dot), 3600 bar (solid line), 4400 bar (long dash), and 5200 bar (solid line). The insets show the corresponding changes in the concentration of the high-spin (triangles), low-spin (circles), and P420 (squares) states of CYP3A4 and the total hemoprotein concentration (diamonds). Conditions as indicated in Fig. 1, except for the concentration of CYP3A4, which was equal 1.9 μM, 2.5 μM, and 1.7 μM for panels ***a***, ***b***, and ***c*** respectively.

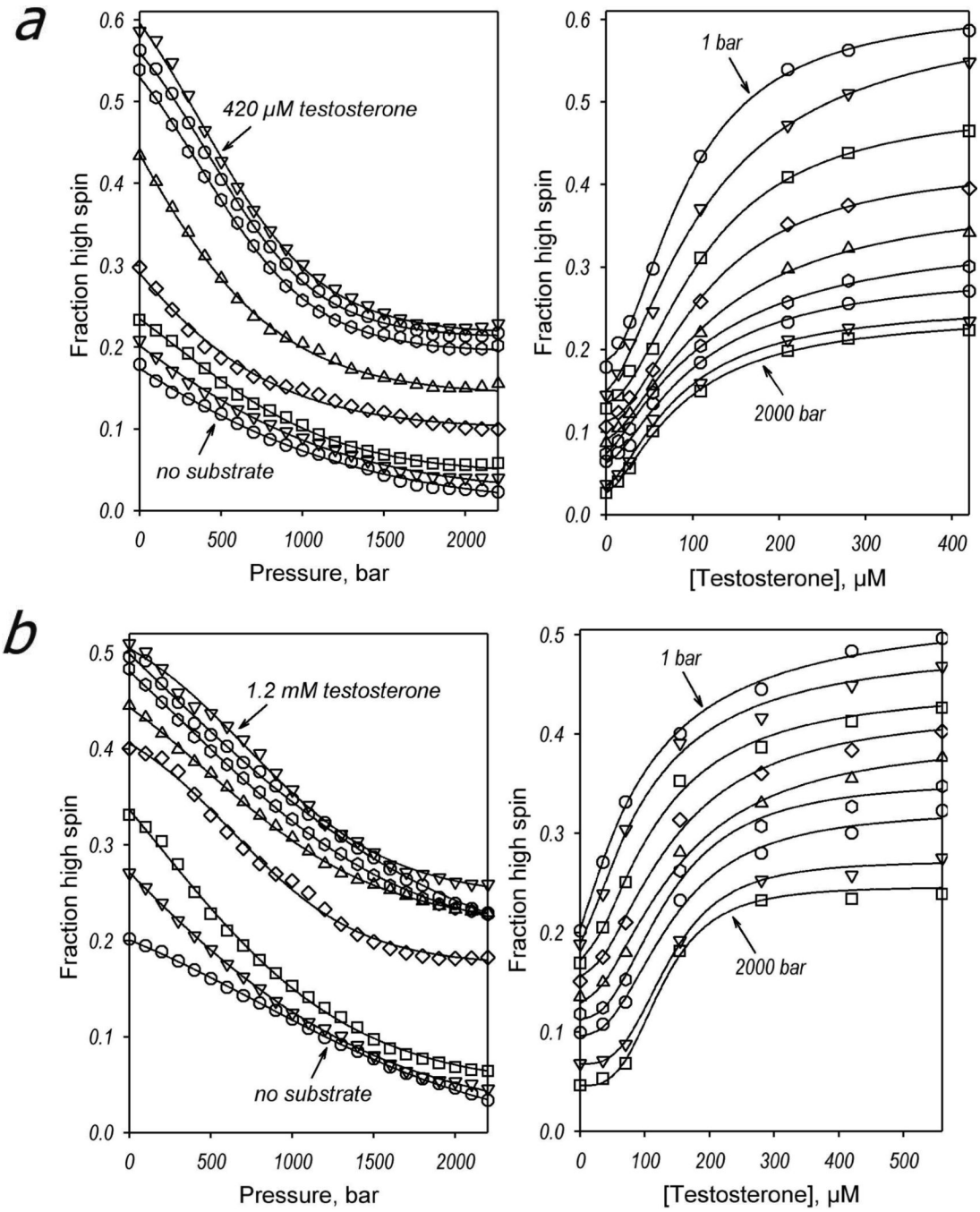

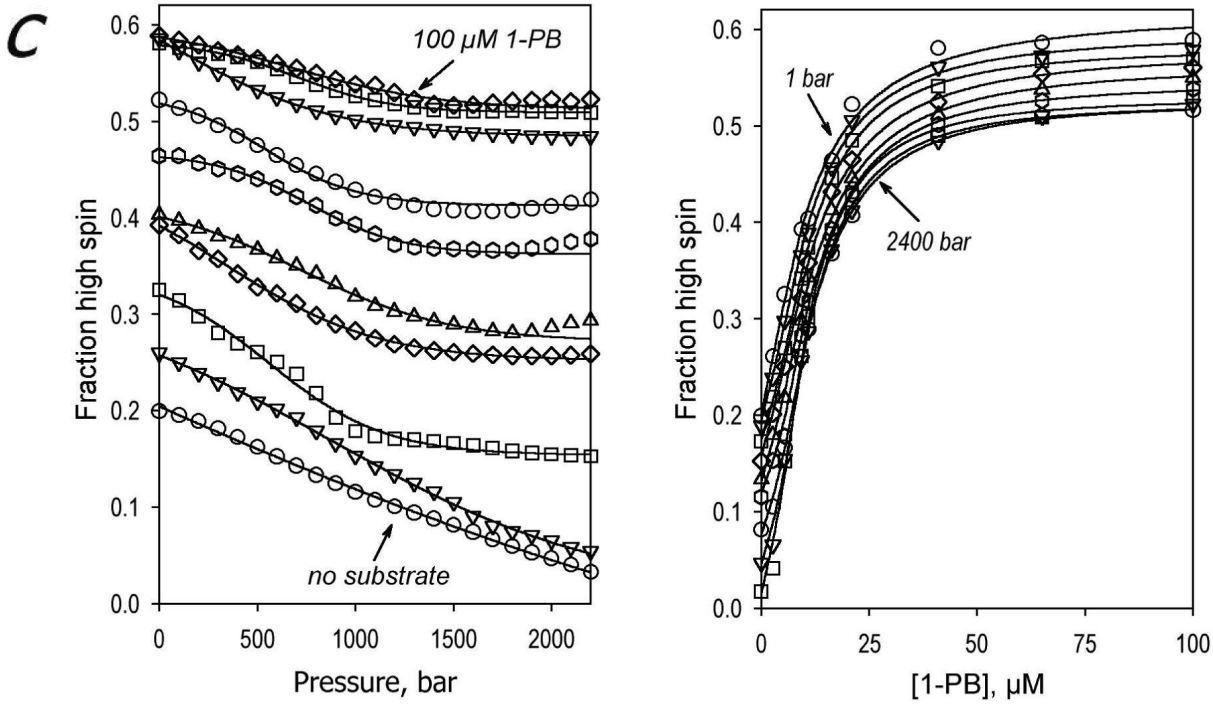

Fig. 7.

Effect of hydrostatic pressure on the spin state of CYP3A4 at increasing concentrations of allosteric substrates. Panel (***a***) illustrates the behavior of CYP3A4ND with testosterone (TST), while panels ***b*** and ***c*** represent the transitions observed with CYP3A4 in solution in the presence of testosterone and 1-PB, respectively. Left panels show the dependencies of the high spin content on pressure at various concentration of substrates. Solid lines represent the results of fitting of these curves to eq. 3. The curves shown in the panel ***a*** correspond to no substrate added, and 14, 28, 56, 112, 210, 280, and 420 μM testosterone. The data shown in the panel ***b*** represent the dependencies obtained at no substrate added, and 35, 70, 154, 280, 420, 560, and 1225 μM testosterone. The data represented in panel ***c*** correspond to no substrate added, and 2.7, 5.4, 9.3, 11, 16, 21, 41 and 100 μM 1-PB. Right panels show the same data set as the dependencies of the high spin content on the substrate concentration at a series of hydrostatic pressures increasing from 1 bar to 1600 bar in 200 bar and at 2000 bar. The curves obtained at 800, 1200 and 1400 bars are omitted from panel ***c*** for clarity. Solid lines show the results of fitting of the titration curves to the Hill equation. Conditions as indicated in Fig. 6.

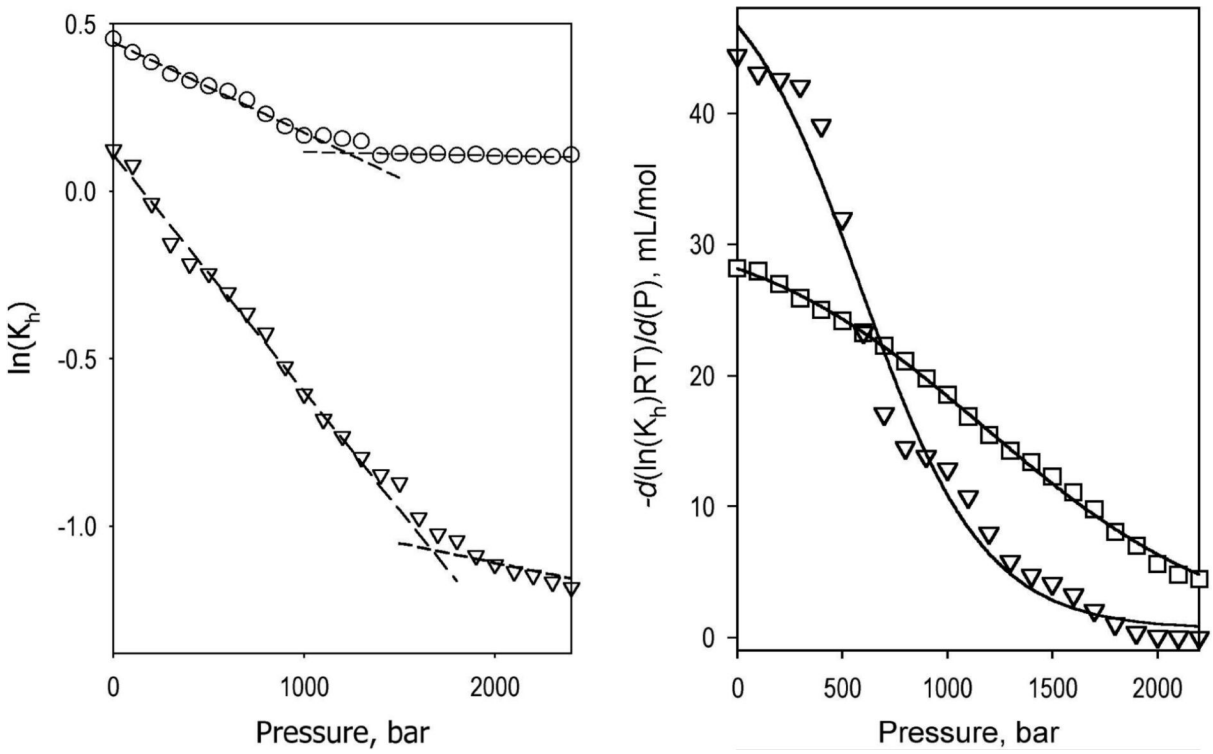

Fig.8.

Effect of hydrostatic pressure on the constant of spin equilibrium for the complexes of CYP3A4ND with testosterone (triangles) and CYP3A4 in solution with either testosterone (squares) or 1-PB (circles). The left panel illustrates the pressure dependencies of the logarithms of $K_{h,S}$, whereas the right panels show the first derivatives of the above dependencies approximated by a 5-th order polynomial. Dashed lines shown in the left panel represent a linear approximation of the initial and final parts of the curves. Solid lines shown in the right panels show the results of fitting of the respective data sets to eq. 3 with the parameters characterized in Table 1. The number of data sets represented in each panel is limited to two for readability of the plots.

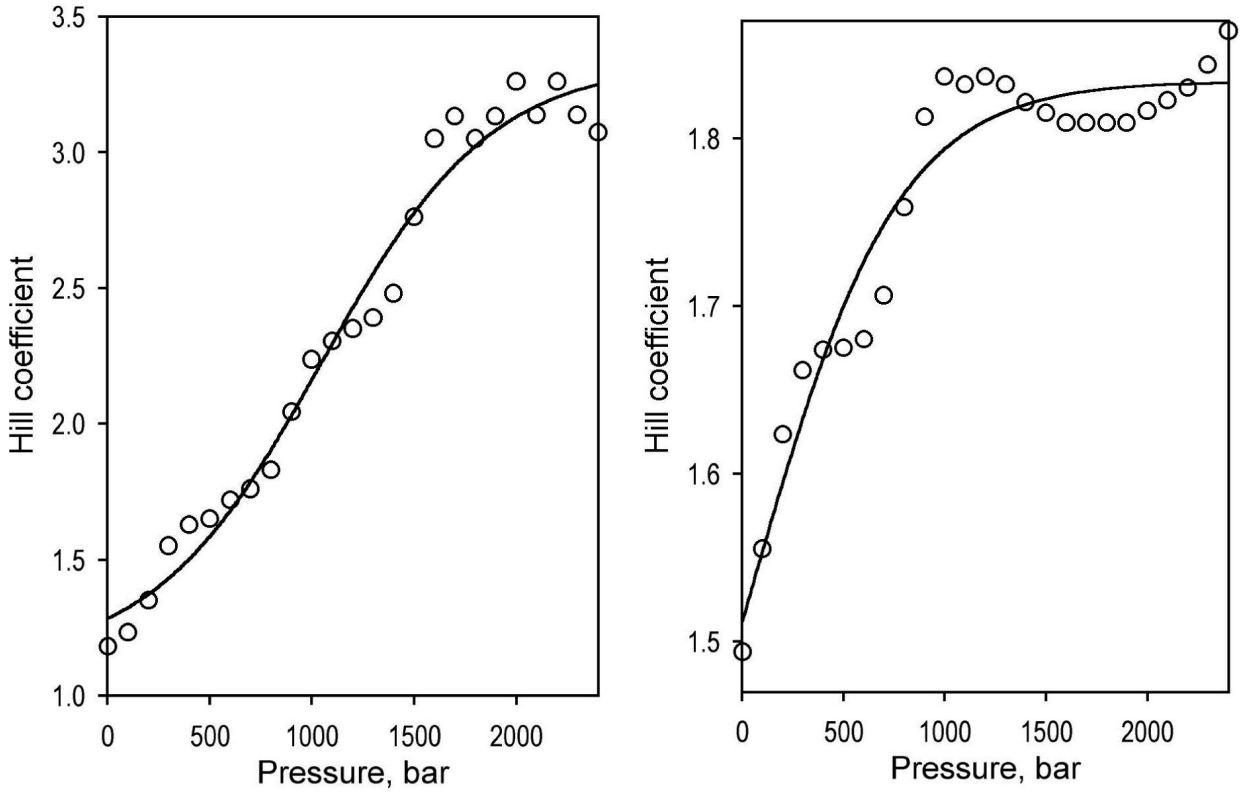

Fig. 9.

Effect of hydrostatic pressure on the cooperativity of interactions of CYP3A4 in solution with testosterone (left) and 1-PB (right). The values of the Hill coefficient at various pressures were obtained from the fitting of the data set shown in Figure 7b and 7c (right panels) to the Hill equation.

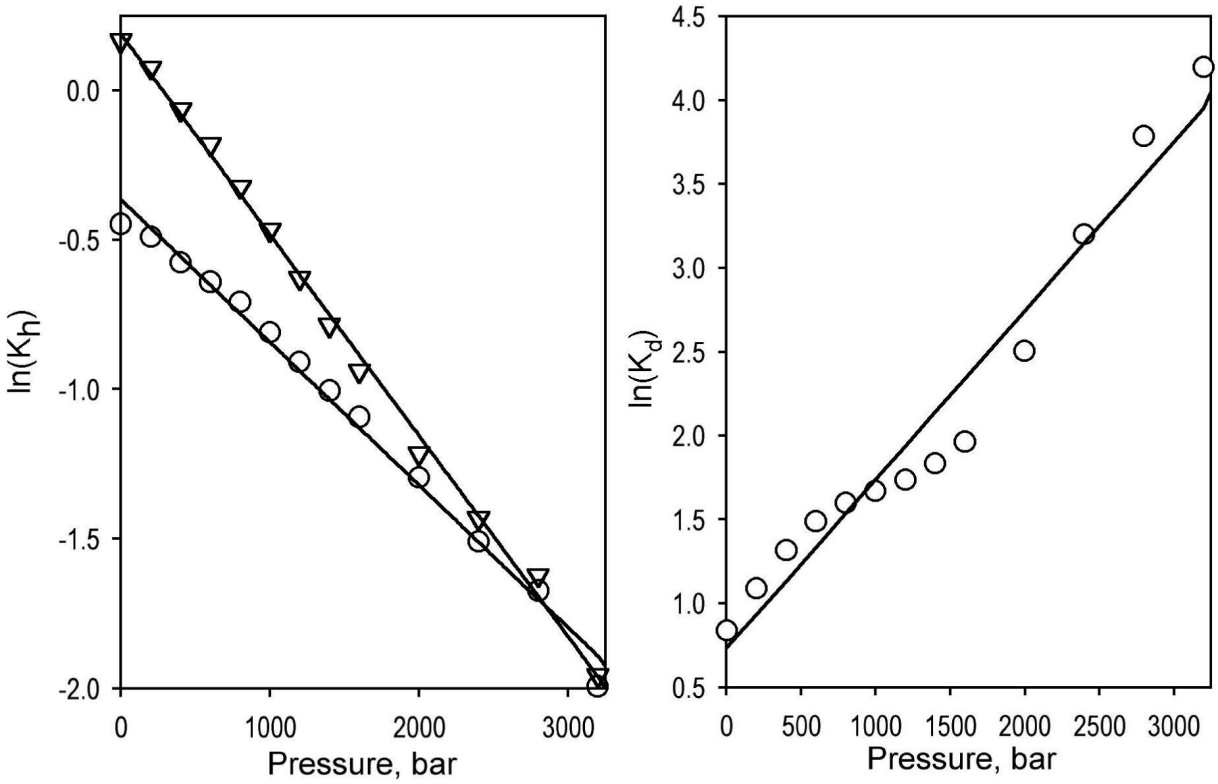

Fig. 10.

The effect of pressure on the parameters of spin transition and substrate dissociation for the interactions of the heme domain of cytochrome P450 BM3 (BMP) with palmitic acid. The data represent the results of fitting of the data taken from our earlier publication (31). Pressure dependencies of the logarithms of constants of spin equilibrium $K_{h,free}$ (circles) and $K_{h,S}$ (triangles) are shown in the left panel. The right panel represents a similar plot for K_D. Solid lines show the linear approximation of the data sets.

Table 1

Parameters of interactions of CYP3A4 with substrates at ambient pressure*

System	Substrate	K_D or S_{50}	n	ΔF_h(max),%[a]
3A4 in solution	BCT	0.31 ± 0.1	N/A	33 ± 6
	testosterone	88 ± 16	1.21 ± 0.04	36 ± 3
	1-PB	10.6 ± 0.7	1.55 ± 0.2	42 ± 8
3A4-ND	BCT	0.39 ± 0.2	N/A	51 ± 18
	testosterone	100 ± 8	1.62 ± 0.2	46 ± 3

* The values represent the averages of the results of 3−6 individual absorbance titration experiments at ambient pressure. In the titrations with testosterone and 1-PB stock solutions of the complexes of the substrates with HPCD in 0.1 M Na-Hepes buffer, pH 7.4 were used (see Materials and Methods).

[a] Maximal amplitude of substrate-induced spin shift, %.

Table 2

Parameters of pressure dependent equilibria in CYP3A4

Substrate	System	ΔV^{o}_{spin}, mL/mol		ΔV^{o}_{diss}, mL/mol		Parameters of R→P transition[a]			
						Based on pressure dependence of K_h		Based on pressure dependence of K_d (S_{50})	
		R-state	P-state	R-state	P-state	$\Delta V^{o}_{R\rightarrow P}$, mL/mol	$K_{R\rightarrow P}$ at 1 bar	$\Delta V^{o}_{R\rightarrow P}$, mL/mol	$K_{R\rightarrow P}$ at 1 bar
None	3A4ND	14	58	N/A	N/A	−69	0.04	N/A	N/A
	3A4 in solution	10	27	N/A	N/A	−54	0.09	N/A	N/A
BCT	3A4ND	7.4	38	−74	0.7	−69	0.04	−98	0.04
	3A4 in solution	11	36	−31	78	−91	0.01	−77	0.01
testosterone	3A4ND	34	−5	0	0	−52	0.3	N/A	N/A
	3A4 in solution	32	0	−15	11	−42	0.13	−45	0.16
1-PB	3A4 in solution	9.1	−1	−6.7	8.5	−58	0.07	−52	0.07

[a] Barotropic parameters of the R→P transition obtained from the fitting of the first derivative plots for $\ln(K_h)$, $\ln(K_d)$ or $\ln(S_{50})$ to eq. 3. Values of the constant of R↔P equilibrium were derived from the corresponding $P_{1/2}$ and ΔV^{o} values according to eq. 2.